Photochemical origin of SiC_2 in the circumstellar envelope of carbon-rich AGB stars revealed by ALMA

Feng, Y., Li, X., Millar, T. J., Szczerba, R., Wang, K., Quan, D., Qin, S., Fang, X., Tuo, J., Miao, Z., Ma, R., Xu, F., Sun, J., Jiang, B., Chang, Q., Yang, J., Hou, G. L., Li, F., & Zhang, Y. (2023). Photochemical origin of SiC_2 in the circumstellar envelope of carbon-rich AGB stars revealed by ALMA. *Frontiers in Astronomy and Space Sciences*, *10*, Article 1215642. https://doi.org/10.3389/fspas.2023.1215642

Published in:
Frontiers in Astronomy and Space Sciences

Document Version:
Publisher's PDF, also known as Version of record

Queen's University Belfast - Research Portal:
Link to publication record in Queen's University Belfast Research Portal

Publisher rights
Copyright 2023 the authors.
This is an open access article published under a Creative Commons Attribution License (https://creativecommons.org/licenses/by/4.0/), which permits unrestricted use, distribution and reproduction in any medium, provided the author and source are cited

General rights
Copyright for the publications made accessible via the Queen's University Belfast Research Portal is retained by the author(s) and / or other copyright owners and it is a condition of accessing these publications that users recognise and abide by the legal requirements associated with these rights.

Take down policy
The Research Portal is Queen's institutional repository that provides access to Queen's research output. Every effort has been made to ensure that content in the Research Portal does not infringe any person's rights, or applicable UK laws. If you discover content in the Research Portal that you believe breaches copyright or violates any law, please contact openaccess@qub.ac.uk.

Open Access
This research has been made openly available by Queen's academics and its Open Research team. We would love to hear how access to this research benefits you. – Share your feedback with us: http://go.qub.ac.uk/oa-feedback

Download date:10. Jul. 2024

frontiers | Frontiers in Astronomy and Space Sciences

TYPE Original Research
PUBLISHED 14 August 2023
DOI 10.3389/fspas.2023.1215642

OPEN ACCESS

EDITED BY
Malgorzata Biczysko,
Shanghai University, China

REVIEWED BY
Claudio Codella,
Osservatorio Astrofisico di Arcetri (INAF), Italy
Dipen Sahu,
Physical Research Laboratory, India

*CORRESPONDENCE
Xiaohu Li,
✉ xiaohu.li@xao.ac.cn

RECEIVED 02 May 2023
ACCEPTED 20 July 2023
PUBLISHED 14 August 2023

CITATION
Feng Y, Li X, Millar TJ, Szczerba R, Wang K, Quan D, Qin S, Fang X, Tuo J, Miao Z, Ma R, Xu F, Sun J, Jiang B, Chang Q, Yang J, Hou G-L, Li F and Zhang Y (2023), Photochemical origin of SiC_2 in the circumstellar envelope of carbon-rich AGB stars revealed by ALMA. *Front. Astron. Space Sci.* 10:1215642. doi: 10.3389/fspas.2023.1215642

Photochemical origin of SiC_2 in the circumstellar envelope of carbon-rich AGB stars revealed by ALMA

Yanan Feng[1,2], Xiaohu Li[1,3]*, Tom J. Millar[4], Ryszard Szczerba[5], Ke Wang[6], Donghui Quan[1,7], Shengli Qin[1,8], Xuan Fang[1,9,10,11], Juan Tuo[1,2], Zhenzhen Miao[1], Rong Ma[1,2], Fengwei Xu[6,12], Jingfei Sun[1], Biwei Jiang[13,14], Qiang Chang[15], Jianchao Yang[1,2], Gao-Lei Hou[16], Fangfang Li[1] and Yong Zhang[1,11,17]

[1]Xinjiang Astronomical Observatory, Chinese Academy of Sciences, Urumqi, China, [2]School of Astronomy and Space Science, University of the Chinese Academy of Sciences, Beijing, China, [3]Key Laboratory of Radio Astronomy, Chinese Academy of Sciences, Urumqi, China, [4]Astrophysics Research Centre, School of Mathematics and Physics, Queen's University Belfast, Belfast, United Kingdom, [5]Nicolaus Copernicus Astronomical Center, Polish Academy of Sciences, Warsaw, Poland, [6]The Kavli Institute for Astronomy and Astrophysics at Peking University (KIAA-PKU), Beijing, China, [7]Research Center for Intelligent Computing Platforms, Zhejiang Laboratory, Hang Zhou, China, [8]Department of Astronomy, Yunnan University, Kunming, China, [9]National Astronomical Observatories, Chinese Academy of Sciences, Beijing, China, [10]Department of Physics, Faculty of Science, The University of Hong Kong, Hang Zhou, China, [11]Laboratory for Space Research, Faculty of Science, The University of Hong Kong, Hang Zhou, China, [12]Department of Astronomy at Peking University (DoA-PKU), Beijing, China, [13]Institute for Frontiers in Astronomy and Astrophysics, Beijing Normal University, Beijing, China, [14]Department of Astronomy, Beijing Normal University, Beijing, China, [15]School of Physics and Optoelectronic Engineering, Shandong University of Technology, Zibo, China, [16]MOE Key Laboratory for Non-Equilibrium Synthesis and Modulation of Condensed Matter, School of Physics, Xi'an Jiaotong University, Xi'an, China, [17]School of Physics and Astronomy, Sun Yat-sen University, Guangzhou, China

The fact that whether SiC_2 is a parent species, formed in the photosphere or as a by-product of high-temperature dust formation, or a daughter species, formed in chemistry driven by the photodestruction of the parent species in the outer envelope, has been debated for a long time. In this study, we analyze the Atacama Large Millimeter Array (ALMA) observations of four SiC_2 transitions in the circumstellar envelopes (CSEs) of three C-rich asymptotic giant branch (AGB) stars (AI Vol, II Lup, and RAFGL 4211) and find that SiC_2 exhibits an annular, shell-like distribution in these targets, suggesting that SiC_2 can be a daughter species in the CSEs of carbon-rich AGB stars. The results may provide important references for future chemical models.

KEYWORDS

asymptotic giant branch stars, mass loss, circumstellar envelope, C-rich, SiC_2, AI Vol, II Lup, RAFGL 4211

1 Introduction

Late evolutionary stars with masses between 0.8 and 8 $M_\odot$ (Höfner and Olofsson, 2018) experience dramatic mass losses. The stellar wind continues to eject material outward, eventually forming a circumstellar envelope (CSE), often referred to as the molecular space factory. According to different C/O ratios, asymptotic giant branch (AGB) stars are divided into three classes: O-rich AGB stars (oxygen-rich, C/O < 1), S-type AGB stars (C/O ≈ 1), and C-rich AGB stars (carbon-rich, C/O > 1). Over 105 molecular species have been detected in the circumstellar envelope of the evolved stars (Decin, 2021). These species, distributed in different areas of CSEs, can help us trace shell properties, such as local temperature and gas composition, and help us understand the chemical synthesis within the objects. A large number of carbon-bearing species are observed in abundance surrounding the carbon stars, for instance, CO, CS, HC_3N, and C_2H, some of which come from the inner layers of CSEs, while some are formed in the outer regions (Decin et al., 2008; Li et al., 2016).

Silacyclopropynylidene (SiC_2) was first detected and confirmed in IRC +10216 by Thaddeus et al. (1984), who derived a fairly large column density, 1.5 × 10^{14} cm^{-2}. Glassgold et al. (1986) suggested that SiC_2 was formed by the reaction of Si^+ with C_2H_2 or C_2H, followed by dissociative recombination with electrons. Glassgold et al. (1991) suggested alternative pathways, initiated by reactions of SiS with $C_2H_2^+$ or $C_2H_3^+$. All these routes need the presence of UV photons to form cations and radicals and, thus, treat SiC_2 as a daughter species.

The spatial distribution of SiC_2 in IRC +10216 was discussed by Takano et al. (1992) and Guelin et al. (1993), who showed a spherical shell-like structure indicative of a daughter species. Lucas et al. (1995) and Gensheimer et al. (1995) used the Plateau de Bure and the Berkeley–Illinois–Maryland Array (BIMA), respectively, to map SiC_2 emissions, showing that it had a shell structure. The first confirmation that SiC_2 was present close to the star came from Cernicharo et al. (2010), who used the Herschel Space Observatory to detect some 55 transitions from energy levels 500–900 K above the ground state, implying that SiC_2 was present in the dust-forming zone. Subsequently, Fonfría et al. (2014), using the CARMA interferometer, and Prieto et al. (2015), using the Atacama Large Millimeter Array (ALMA), detected emissions from both the central region and the outer shell.

In a work devoted to single-dish observations of 25 C-rich AGB stars (Massalkhi et al., 2018), SiC_2 and SiC were detected in about half of the sources. They found that the abundance of SiC_2 decreased with the increasing envelope density, indicating that SiC_2 is a parent species in these CSEs. De Beck and Olofsson (2020) detected SiC_2 in the S-type AGB star W Aql, and showed that the emission occurs in a ring of a radius of 1–2″.

Most evidence shows that SiC_2 is formed in LTE conditions close to the star, although IRC +10216 has an increase in the abundance of SiC_2 at approximately 10″, indicating an additional formation in the outer regions of CSEs. To date, no millimeter-wave interferometric array observation of SiC_2 has been published in CSEs of C-rich AGB stars other than IRC +10216. In this work, we provide evidence that SiC_2 seems to be a daughter molecule through high-resolution observations of three C-rich AGB stars. We describe the observations in Section 2. The results are discussed in Section 3. The conclusion is presented in Section 4. The spatial distribution and the fractional abundance of SiC_2 in AI Vol together with $5_{0,5} - 4_{0,4}$ transitions in RAFGL 4211 are discussed in the main paper, while the rest of the results are presented in the Supplementary Material.

2 Observations

Observations were made using the ALMA 12-m array. The spectral line observations in three bands of AI Vol, RAFGL 4211, and II Lup covering four Windows with a bandwidth of 2 GHz were performed on 16 August 2015 (2013.1.00070.S, PI: Nyman, Lars-Åke). The data were extracted from the ALMA Archive[1]. For AI Vol, the configuration used for the observation is a 12-m main array, with baselines 21–783 m. The image cube per spw averages every 2 × 488 kHz channel. The rms requirement is 3 mJy per 1 arcsec beam, per 0.9 MHz (~2.7 km s^{-1}). The synthesized rms is 1.3 mJy/beam, and the synthesized beam is 1.4″× 0.9″. The parameters of the observed transitions are shown in Table 1. The frequency resolution during the observation is 1,128.9984 kHz, corresponding to the velocity resolution of 2.526–3.122 km s^{-1}. The wide frequency range covers four lines of SiC_2 ($4_{0,4} - 3_{0,3}$, $4_{2,3} - 3_{2,2}$, $4_{2,2} - 3_{2,1}$, and $5_{0,5} - 4_{0,4}$).

AI Vol, RAFGL 4211, and II Lup are all carbon-rich AGB stars with mass losses. A survey conducted by Smith et al. (2015) at the 3-mm band revealed that the three carbon-rich stars possess abundant molecules but the sensitive detection of molecular spatial distributions relies on more advanced telescopes, such as ALMA. In this study, we present the physical parameters taken from the literature and the synthesized beam for the observed sources, which are listed in Table 2.

The imaging process of the calibrated data was manually performed using CASA 4.3.1[2] software. The "clean" task was employed, and to achieve a balance between the spatial resolution and noise gain in the resulting image, the Briggs weighting function was applied along with adjustments to the "robust" parameter of 0.5. The rms was calculated near the center of the field, excluding all emissions within the region. The rms values for all channel maps were obtained using the task "imstat" in CASA software. Each pixel on the image plane corresponded to a size of 0.2 arcseconds. Then, we used Python software to map and analyze ALMA product data. To calculate the molecular column density, we employed shell fitting using GILDAS software[3], along with Splatalogue[4] and CDMS databases[5] (Müller et al., 2005).

3 Result

3.1 Spatial distribution of SiC_2

We found four transitions of SiC_2 from each source, except for the $4_{2,2} - 3_{2,1}$ transition, which was not observed in II Lup. Based on $S\mu^2$ from Table 3, the $4_{2,2} - 3_{2,1}$ transition of SiC_2 in the 3-mm wavelength range ranked third in terms of signal intensity. However, we did not detect any signal. Our data were obtained from the ALMA Archive, and from the data information, we found that the other

---

[1] https://almascience.nao.ac.jp/aq

[2] https://casa.nrao.edu/

[3] http://www.iram.fr/IRAMFR/GILDAS

[4] https://splatalogue.online//advanced.php

[5] http://www.astro.uni-koeln.de/cdms/catalog

TABLE 1 Spectral line parameters of different transitions in SiC_2 obtained via shell fitting using GILDAS.

Transition	Frequency (GHz)	AI Vol				RAFGL 4211				II Lup			
		rms (mK)	$\int T_R dv$ (K km s^{-1})	T_{peak} (K)	S/N	rms (mK)	$\int T_R dv$ (K km s^{-1})	T_{peak} (K)	S/N	rms (mK)	$\int T_R dv$ (K km s^{-1})	T_{peak} (K)	S/N
$J_{Ka,\,Kc} = 4_{0,\,4}{-}3_{0,\,3}$	93.06363900	6.70	1.26 (±0.21)	0.14	20.45	16.40	1.48 (±0.52)	0.14	8.60	21.49	9.51 (±0.75)	0.54	25.11
$J_{Ka,\,Kc} = 4_{2,\,3}{-}3_{2,\,2}$	94.24539300	2.73	0.29 (±0.09)	0.03	10.99	10.70	0.53 (±0.34)	0.06	5.51	25.13	6.82 (±0.88)	0.37	14.82
$J_{Ka,\,Kc} = 4_{2,\,2}{-}3_{2,\,1}$	95.57938100	2.55	0.32 (±0.08)	0.04	13.73	16.30	0.91 (±0.52)	0.10	6.13	47.30	–	–	–
$J_{Ka,\,Kc} = 5_{0,\,5}{-}4_{0,\,4}$	115.38238880	6.64	0.48 (±0.21)	0.04	5.27	40.60	4.45 (±1.30)	0.33	8.08	72.80	17.20 (±2.55)	0.80	11.03

Note: the uncertainties are indicated in parentheses. S/N is calculated by T_{peak}/rms.

three transitions of SiC_2 and the data from two additional sources had map sizes of 800 × 800 or 640 × 640 pixels. In contrast, the data without signal detection only covered a map size of 300 × 300 pixels. We speculate that there may have been some unknown special circumstances during the observations that led to the absence of a signal.

AI Vol does not have the strongest spectral line signal, but the signal-to-noise ratio of the spatial brightness distribution is higher than that of the other two stars. Cernicharo et al. (2015) have reported the observations and model results of a C-rich AGB star, IRC +10216. They suggest that a companion star may explain the spiral structure of its CSE. Lykou et al. (2018) reported spiral structures of several parent molecules in II Lup, suggesting that a companion star is the main forming mechanism of mass loss. The results show that the spectral line signal of AI Vol is stronger than RAFGL 4211 (in Figure 6; Supplementary Figure SA9). In order to get reliable results, we concentrate on analyzing the distribution around the center star of AI Vol (in Section 3.1.1). The rotational diagram method was used to calculate fractional abundance, and its detailed analysis is presented in Section 3.2.

3.1.1 AI Vol

Figures 1, 2 show the SiC_2 ($4_{0,\,4} - 3_{0,\,3}$ and $4_{2,\,2} - 3_{2,\,1}$) radial velocity channel map toward the C-rich AGB star AI Vol (the other transitions are shown in Supplementary Figures SA1, A2). Around the local standard of the rest velocity V_{LSR} of AI Vol (−39 km s^{-1}), SiC_2 shows a ring distribution around the center star with a diameter of ~4–6″ (~2,840.95–4,258.08 au), and the signal strength reaches 20.4 and 13.7σ for $4_{0,\,4} - 3_{0,\,3}$ and $4_{2,\,2} - 3_{2,\,1}$ transitions. Based on the images presented by Decin et al. (2015), it is evident that the parent molecules, such as SiO, exhibit a concentrated distribution within a compact structure surrounding the central star. In contrast, our observation reveals a characteristic pattern specific to the daughter molecules, distributed in hollow rings around the star (Agúndez et al., 2015; 2017). The brightness distributions of Figures 1, 2 under different velocity components are all generated from the transitions ($4_{0,\,4} - 3_{0,\,3}$ and $4_{2,\,2} - 3_{2,\,1}$) without the spatial extension caused by the fine structure.

The brightness distribution of the $4_{0,\,4} - 3_{0,\,3}$ transition of SiC_2 and the 2–1 transition of SiO around V_{LSR} channels (from 32.3 to 46.5 km s^{-1}) are shown in Figure 3. We can see that the maximum emission of SiC_2 occurs at the radius of ~3″, with a hole in the distance from the star ~2″. The studies conducted by Takano et al. (1992) and Agúndez et al. (2015) showcased the spatial distribution of the daughter species centered around V_{LSR}. SiO is present as the parent species in three types of AGB stars (Cherchneff, 2006; Ramstedt et al., 2009). SiC_2 and SiO, shown in Figure 3, represent the spatial distribution characteristics of the daughter species and parent species, respectively, exhibiting distinct hollow and compact structures.

The northeast part of the shell emission has relatively stronger spectral signals. The SiC_2 ($4_{0,\,4} - 3_{0,\,3}$) transition for AI Vol is stronger than the other transitions, and the hollow shell structure can be seen more clearly. SiC_2 at different velocity components showed an elongated cavity extending from the inner region to a location with a southern radius of ~2″. This structure may be

TABLE 2 Source and observational parameters.

Name	IRAS	Mass loss rate ($M_\odot$yr^{-1})	Distance (pc)	V_{LSR} (km s^{-1})	V_{exp} (km s^{-1})	θ$_{beam}$ (″)
AI Vol	IRAS 07454-7112	4.9(−6)$^{(2)}$	710$^{(2)}$	−39.0$^{(2)}$	12.0$^{(2)}$	1.51 × 0.99$^{(1)}$
RAFGL 4211	IRAS 15082-4808	1.0(−5)$^{(3)}$	850$^{(4)}$	−3.0$^{(5)}$	19.5$^{(3)}$	1.00 × 1.00$^{(1)}$
II Lup	IRAS 15194-5115	1.7(−5)$^{(2)}$	500$^{(2)}$	−15.5$^{(2)}$	21.5$^{(2)}$	0.75 × 0.45$^{(1)}$

Note: $a(b) = a \times 10^b$. Mass loss, distance, local standard of rest (V_{LSR}), and expansion (V_{exp}) velocities from the literature and synthesized beam, θ_{beam}. References: (1)this work; (2)Danilovich et al. (2018); (3)Woods et al. (2003); (4)Groenewegen et al. (2002); (5)Smith et al. (2015).

TABLE 3 Upper energy, E_u, and $S\mu^2$ of molecular SiC$_2$ in the observed transitions extracted from the "Splatalogue" database.

Transition	E_u (K)	$S\mu^2$ (Debye^2)
$J_{Ka,\,Kc} = 4_{0,\,4}{-}3_{0,\,3}$	11.23	22.82
$J_{Ka,\,Kc} = 4_{2,\,3}{-}3_{2,\,2}$	19.12	17.18
$J_{Ka,\,Kc} = 4_{2,\,2}{-}3_{2,\,1}$	19.22	17.18
$J_{Ka,\,Kc} = 5_{0,\,5}{-}4_{0,\,4}$	16.77	28.46

caused by a companion star, but AI Vol has no spiral structure typical of a companion star (Cernicharo et al., 2015). The gas expands at a lower velocity near the star, and lower-excited state transitions farther from the star are more spatially distributed than higher-excited state transitions of the same source. This is seen in Figure 4, where the zeroth-order moment map of the ($5_{0,\,5} - 4_{0,\,4}$) transition has a smaller extent than the ($4_{0,\,4} - 3_{0,\,3}$) transition.

The difference between Figures 3, 4 lies in their representation of data. In Figure 3, we present channel maps which provide images of vertical slices through the expanding envelope, while Figure 4 shows the line intensity integrated over all velocities. From Figure 3, we can see the clear feature of SiC$_2$ as a daughter molecule. Figure 4 offers a broader perspective by showcasing the distribution of all signals. Moreover, it reveals that the gas intensity spatial distribution of AI Vol for different transitions varies in size. Compared to transitions with low rotational quantum numbers, transitions with high rotational quantum numbers are distributed closer to the star.

The inner region of AGB stars is at $\lesssim 20R_*$ (3.89×10^{14} cm), and the intermediate area of the CSE of AI Vol is at $\lesssim 70R_*$ (1.36×10^{15} cm) (Decin et al., 2008). So the radius of SiC$_2$ molecules in AI Vol coincides with the region of the daughter species in the model (Li et al., 2016).

3.1.2 RAFGL 4211 and II Lup

Figure 5; Supplementary Figures SA3–A5 show the channel maps of the four transitions of SiC$_2$ for RAFGL 4211. The synthesized beam of observation is 1.00 ×1.00″, with position angles (PA) 0°. Signal strengths range from 5σ to 8σ. The brightness distribution radius is ~5″ at approximately V_{LSR} = −3.0 km s^{-1} velocity (distance from the star center to peak intensity). A hollow shell structure exists within the radius ~3″ of the star. The SiC$_2$ spatial distribution range of RAFGL 4211 is found to be ~6.36×10^{16}–8.90×10^{16} cm. In addition to focusing on the brightest component, we see some clump distributions in the outer regions.

Supplementary Figures SA6–A8 show the channel map of the three transitions of II Lup. The emissions $4_{2,\,2} - 3_{2,\,1}$ have no notable signals and linewidths (the third panel at the bottom of Supplementary Figure SA9). The synthesized beam of observation is 0.75 × 0.45″. The signal strengths range from 6σ to 11σ. Supplementary Figure SA8 shows that $5_{0,\,5} - 4_{0,\,4}$ emission has the form of a ring around the central position. The brightness distribution radius of the II Lup near V_{LSR} = 15.5 km s^{-1} velocity is ~10″. The SiC$_2$ spatial distribution range of II Lup is found to be ~3.74×10^{16}–7.48×10^{16} cm. As with RAFGL 4211, some clumps can be seen at ~16″. These clumps may be a part of a spiral structure caused by a companion star.

3.1.3 Summary of morphology

The SiC$_2$ channel map (Figures 2, 5) of AI Vol and RAFGL 4211 shows distinct daughter species characteristics. The SiC$_2$ radius greater than the $20R_*$ distribution in the three C-rich AGB stars is consistent with the distribution of daughter species in O-rich AGB stars (Li et al., 2014). The distribution in hollow rings of the three sources indicates that SiC$_2$ is formed in the star's outer layer through chemical reactions. This is the same as the ring distribution of SiC$_2$ in IRC +10216 (Takano et al., 1992). Gensheimer et al. (1995) reported that the inner and outer radii of SiC$_2$ of IRC +10216 are mainly distributed in the range of ~ 2× 10^{16}–6×10^{16} cm. In the analyzed observations of three sources, the SiC$_2$ spatial distribution range is approximately 2.12×10^{16}–8.90×10^{16} cm. Altogether, combining the ring brightness distribution of SiC$_2$ obtained in this work, we confirm that SiC$_2$ is the daughter molecule in the CSEs of C-rich AGB stars.

3.2 Abundance

We use the rotational diagram method to estimate the abundance of SiC$_2$, and the spectral line profiles of the four transitions are shown in Figure 6. Using the parameters in Table 1, the molecular excitation temperature and column density are calculated under the assumption of LTE, and the equation is as follows (Zhang et al., 2009; Wang et al., 2014, e.g.):

$$\ln\left(\frac{3kW}{8\pi^3 \nu S\mu^2}\right) = \ln\left(\frac{N}{Q}\right) - \frac{E_u}{kT_{ex}}. \tag{1}$$

Here, N represents the total column density of the molecule, Q represents the partition function, E_u represents the upper-level

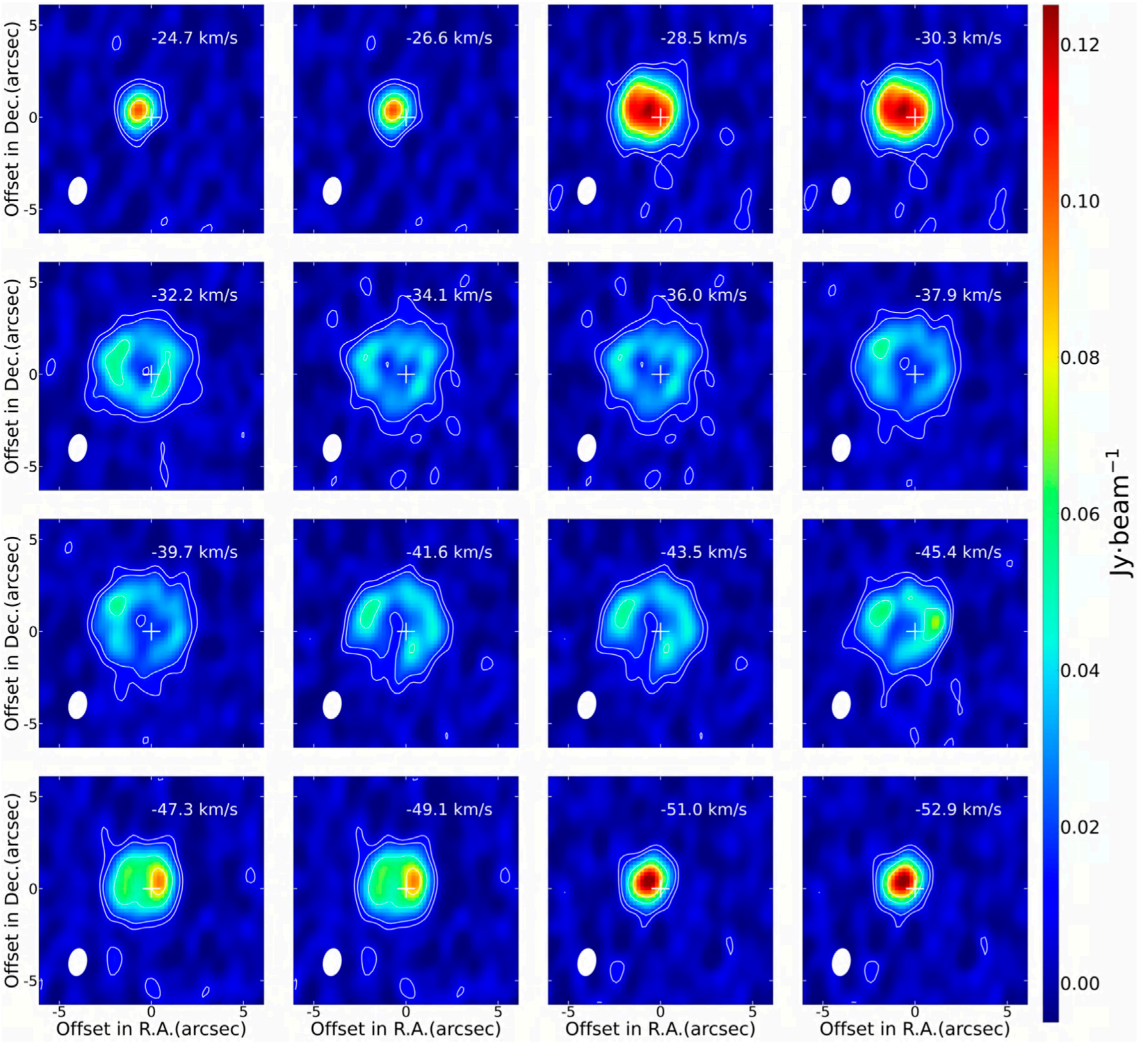

FIGURE 1
Channel maps of SiC_2 ($4_{0,4} - 3_{0,3}$) toward AI Vol. The shape of the synthesized beam is shown in the lower left corner of each panel with a size of 1.51 × 0.99$''$, with PA 9.82°. The systemic velocity is displayed in the top right corner of each panel. The white cross represents the position of the star on the map. The white contour maps display the flux levels of the SiC_2 transition at 5, 10, 30, and 50 times the rms noise, 1σ = 1.6 mJy·beam^{-1}. The selected range of the color bar can show the spatial distribution of molecules better. The brightness distribution of the elongated cavity is similar to that in IRC +10216 (Lucas et al., 1995).

energy, T_{ex} represents the excitation temperature, k represents the Boltzmann constant, υ(Hz) represents the rest frequency, W ($\int T_R d\upsilon$) represents the spectral line integral intensity, and $S\mu^2$ represents the product of the line strength and the square of the electric dipole moment. The values of $S\mu^2$ and E_u/k are taken from the Splatalogue database[6]. As the upper energy levels are close in temperature, the errors in the derived quantities are rather large.

In order to determine the relative abundance of SiC_2 to H_2, it is necessary to evaluate the average H_2 column density within the radius occupied by SiC_2. This can be achieved by employing the following equation (Gong et al., 2015):

$$N_{H_2} = \frac{\dot{M}R/V_{exp}}{\pi R^2 m_{H_2}} = \frac{\dot{M}}{\pi R V_{exp} \mu m_H}. \qquad (2)$$

For AI Vol, $\dot{M} = 4.9 \times 10^{-6}\ M_\odot\ \mathrm{yr}^{-1}$ (Danilovich et al., 2018). R is the radius of the peak of the highest brightness point in Figure 4, which is 3$''$; V_{exp} represents the expansion velocity of 12 km s^{-1} (Nyman and Olofsson, 1995); m_H represents the mass of hydrogen; and μ represents the mean molecular weight of 2.8, as described in Gong et al. (2015). The derived column density of H_2 is 5.52 $\times 10^{20}$ cm^{-2}. In the rotational analysis using Eq. 1, we carried out error propagation and obtained the error of excitation temperature (δT_{ex}) and column density (δN), with the integral intensity of 1σ

---

[6] https://splatalogue.online//advanced.php

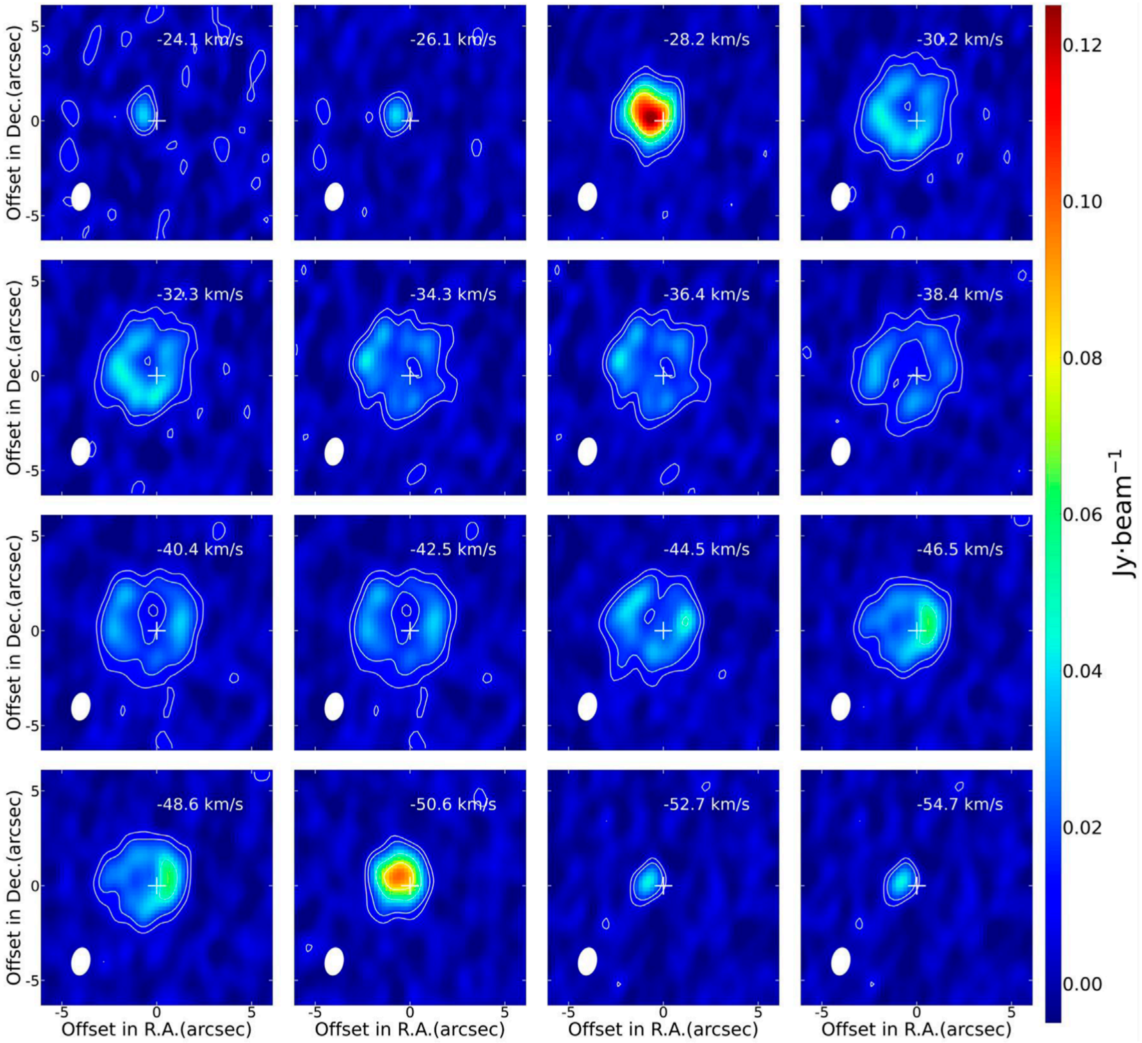

FIGURE 2
Channel maps of SiC_2 ($4_{2,2}-3_{2,1}$) toward AI Vol. The shape of the synthesized beam is shown in the lower left corner of each panel with a size of 1.48 × 0.98″, with PA 10.44°. The velocity (km s^{-1}) is displayed in the top right corner of each panel. The white cross represents the center of the star in the map. The white contours display the flux levels of the SiC_2 transition at 5, 10, 30, and 50 times the rms noise, $1\sigma = 1.5$ mJy·beam^{-1}.

error. The formulas for δT_{ex} and δN are as follows:

$$\delta T_{ex} = \frac{1}{m_R^2}\delta m_R \tag{3}$$

and

$$\delta N = \sqrt{\delta_{N,Q}^2 + \delta_{N_{C_R}}^2}. \tag{4}$$

The slope is represented by m_R, and the intercept is represented by C_R. δN is the uncertainty contribution from the rotation partition function and the intercept of the rotational diagram.

In practical calculations, first, the excited temperature and column density of SiC_2 are fitted by using the rotation diagram method that is described in Eq. 1 and plotted in Figure 7; second, the fractional abundance of SiC_2 is calculated by $f = N/N_{H_2}$. In AI Vol, we obtained $f(SiC_2) = 1.55 \times 10^{-8}$, which is an order of magnitude lower than SiC_2 abundance in IRC +10216, which is approximately 10^{-7} (Cernicharo et al., 2010; Agúndez et al., 2012; Fonfría et al., 2014; Velilla-Prieto et al., 2018). Table 4 presents fractional abundances, column densities, and excitation temperatures of SiC_2 for all three stars. We found that the fractional abundance of SiC_2 increases with the increasing wind density in the three observed C-rich AGB stars.

In the previous astrochemical models of C-rich CSEs of AGB stars, SiC_2 is always treated as a parent species with an initial abundance of $\sim 10^{-5}$ (Li et al., 2014; Massalkhi et al., 2018; Van de Sande and Millar, 2022). However, this study clearly shows that this molecule is a daughter species, and therefore, the chemistry of SiC_2 in chemical models needs to be reinvestigated.

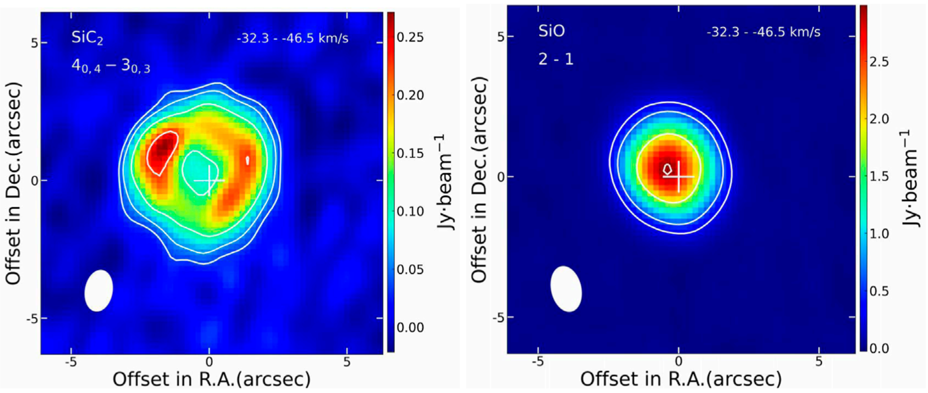

FIGURE 3
Brightness distribution of SiC_2 (left panel) and SiO (right panel) transitions at the source velocity (−32.3––46.5 km s^{-1}) in AI Vol. The color bar shows the brightness distribution of different regions. The white cross represents the center of the star in the map. The beam size of the observation in SiC_2 is 1.51 × 0.99″, with PA 9.82°. The beam size of the observation in SiO is 1.64 × 1.06″, with PA −12.99°. The white contours display the flux levels of SiC_2 at 3, 5, 10, and 20 times the rms noise, with 1σ = 11.3 mJy·beam^{-1}. For SiO (2−1), the flux levels are at 5, 10, 30, and 50 times the rms noise, where 1σ = 58.9 mJy·beam^{-1}.

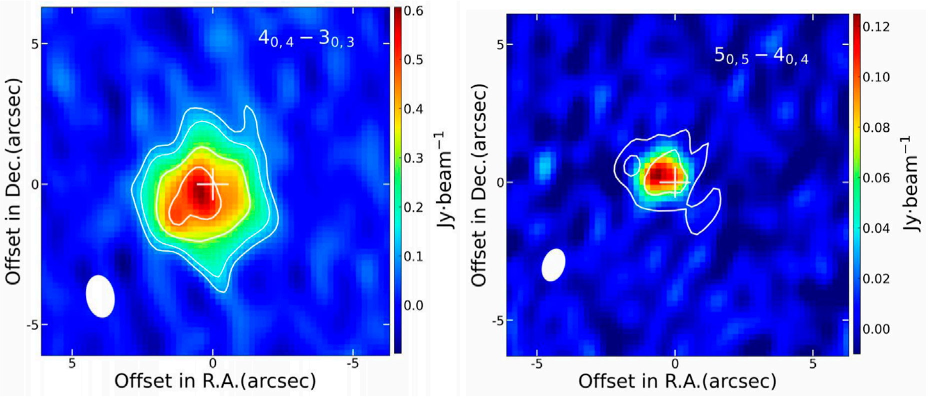

FIGURE 4
Zeroth moment map of the SiC_2 ($4_{0,4} - 3_{0,3}$ and $5_{0,5} - 4_{0,4}$) line at 93.063639 and 115.382375 GHz toward AI Vol. The beam size of observation is 1.51 × 0.99″, with PA 9.82°. The molecular transitions are displayed in the top right corner of each panel. In the right panel, the beam size of observation is 1.20 × 0.79″, with PA 18.86°. In the left panel, the white contours display the flux levels at 3, 5, 10, and 15 times the rms noise, with 1σ = 30.5 mJy·beam^{-1}. In the right panel, the flux levels are shown at 3 and 5σ (1σ = 0.1 mJy·beam^{-1}).

3.3 SiC_2 chemistry

Previous studies on silicon chemistry in CSEs of AGB stars mainly arise from these models constructed for the carbon-rich AGB star IRC +10216. The detailed discussion on the chemistry of the triangular molecule SiC_2 in the inner CSE can be found in Willacy and Cherchneff (1998) and in the outer CSE in Takano et al. (1992), Gensheimer et al. (1995), and MacKay and Charnley (1999), where SiC_2 is found to be mainly formed via ion-neutral reactions and are broken down into SiC due to photodissociation induced by the photons from the interstellar medium. Cernicharo et al. (2010) introduced three key reactions to the formation of SiC_2 (i.e., Si reacts with C_2H_2, Si reacts with C_2H, and Si^+ reacts with C_2H), and then, it can successfully explain the enhanced abundance of SiC_2 from observations. The chemistry of these cyclic molecules is complex. The study of c–SiC_3 by Yang et al. (2019) suggested that the carbon–silicon molecules in the CSE may not only come from complex ion–molecule reactions or the photodissociation of high-molecular weight carbon–silicon molecules but also from bimolecular neutral–neutral reactions, leading to the formation of naked carbon–silicon molecules via photochemical dehydrogenation. Since SiC_2 is likely the gas-phase precursor in forming SiC dust in carbon stars (Massalkhi et al., 2018), the interaction between gas and dust, in addition to the non-spherical and clumpy structures of the envelopes of the stars, will need to be considered in future chemical models.

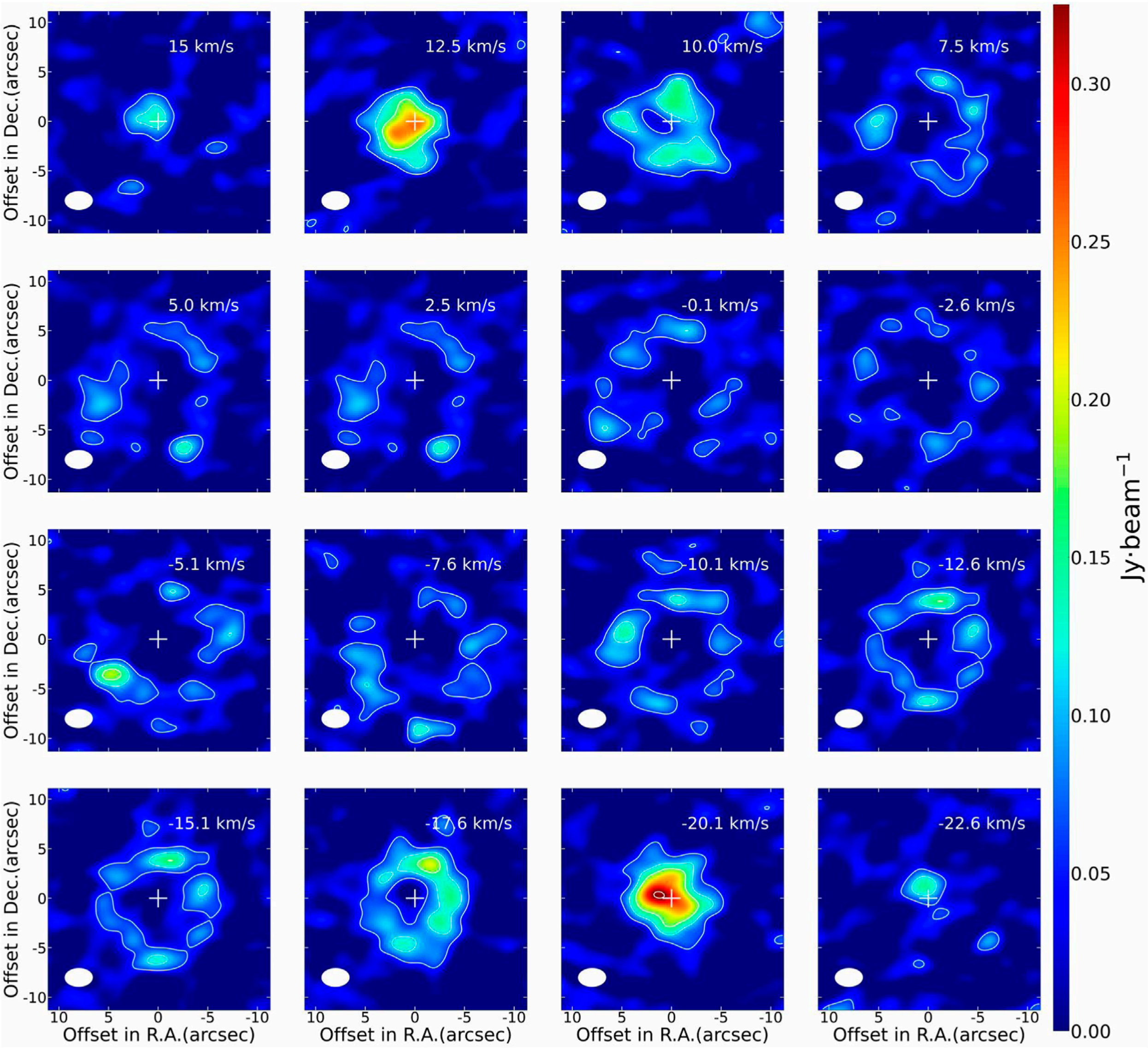

FIGURE 5
Channel maps of SiC_2 ($5_{0,5} - 4_{0,4}$) toward RAFGL 4211. The shape of the synthesized beam is shown in the lower left corner of each panel with a size of 1.40 × 0.93″, with PA 89.13°. The white cross represents the center of the star in the map. The white contours delineate the flux levels of SiC_2, indicating increments of 5, 10, 15, and 30 times the rms noise (1σ = 11.0 mJy·beam^{-1}).

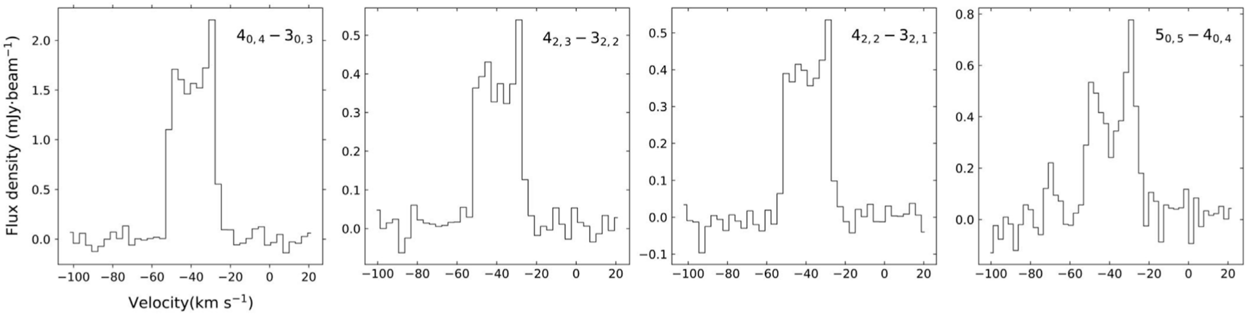

FIGURE 6
Spectral line shapes of SiC_2 toward AI Vol, integrated with a 100 × 100 pixel range centered on the star.

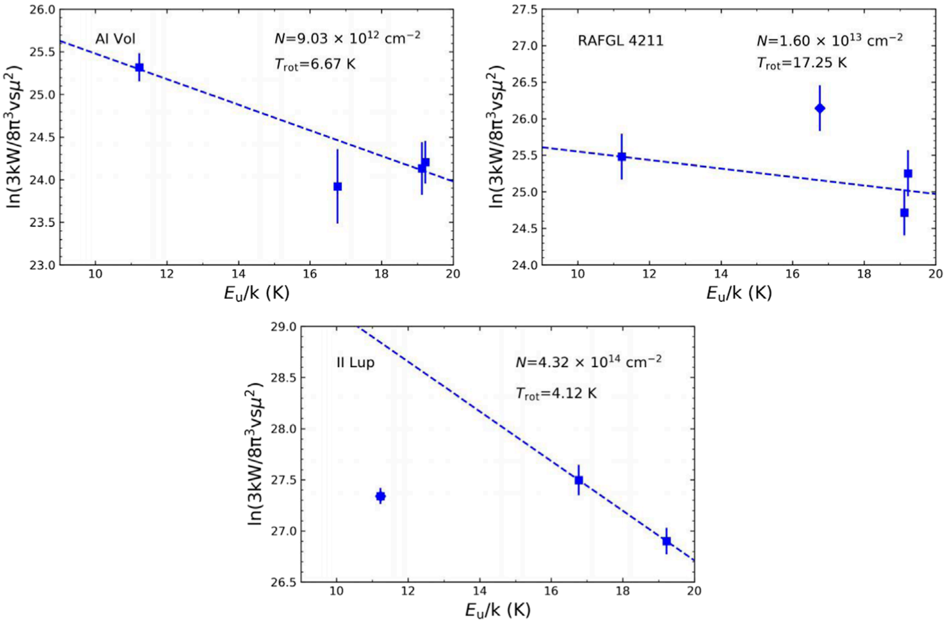

FIGURE 7
Rotational diagram for the observed SiC_2 lines toward AI Vol, RAFGL 4211, and II Lup. The blue dotted lines represent the results from linear least squares fitting by taking into account the weights of the errors. During fitting procedures, the data for SiC_2 transitions of $5_{0,5}-4_{0,4}$ (blue diamond) in RAFGL 4211 and $4_{0,4}-3_{0,3}$ (blue diamond) in II Lup were excluded. The upper right corner in each panel shows the fitted column density and excitation temperature.

TABLE 4 Deduced excitation temperature (T_{ex}), column density (N), and fractional abundance (f) of SiC_2 relative to H_2 in the target sources by the rotational diagram method, along with the previous observational results.

	This work			Other observations			
Source	T_{ex} (K)	$N \times 10^{13}$ (cm^{-2})	$f \times 10^{-8}$	T_{ex} (K)	$N \times 10^{13}$ (cm^{-2})	$f \times 10^{-7}$	$\dot{M}\ /\ V_{exp} \times 10^{-7}$ ($M_{\odot}yr^{-1}$ km^{-1} s)
AI Vol	6.66 (±1.33)	0.90 (±0.49)	1.64	14.00 (±16.00)$^{(b)}$	0.40 (±0.50)$^{(b)}$	2.30$^{(a)}$	4.08$^{(c)}$
RAFGL 4211	17.25 (±13.07)	1.60 (±2.10)	4.62	35.00 (±51.00)$^{(b)}$	4.00 (±3.00)$^{(b)}$	4.90$^{(a)}$	5.13$^{(c)}$
II Lup	4.12	43.22	47.46	19.00 (±11.00)$^{(b)}$	4.00 (±2.00)$^{(b)}$	12.00$^{(a)}$	7.91$^{(a,\ c)}$

Note: $\dot{M}\ /\ V_{exp}$ is proportional to the CSE wind density. The uncertainties are listed in parentheses, which are obtained by considering the 1σ signal via error propagation. The fitting of II Lup was performed using only two data points, which resulted in a lower precision and the absence of error estimation. References: $^{(a)}$Woods et al. (2003); $^{(b)}$Smith et al. (2015); $^{(c)}$Danilovich et al. (2018).

4 Conclusion

To explore whether SiC_2 is a parent or a daughter species, we have analyzed the ALMA observations of SiC_2 ($4_{0,4}-3_{0,3}$, $4_{2,3}-3_{2,2}$, $4_{2,2}-3_{2,1}$, and $5_{0,5}-4_{0,4}$) for the three carbon stars and compared them with SiC_2 results in the C-rich AGB star IRC +10216. The abundance of SiC_2 in the three stars is calculated by the rotational diagram method. Our analysis revealed that SiC_2 molecules in the CSEs of carbon stars exhibited a hollow shell structure, with a distinct brightness distribution at different velocities; therefore, we conclude that SiC_2 exists as a daughter molecule in the CSEs of these sources. Our results are in contrast to some previous reports which concluded that SiC_2 is a parent molecule in the envelopes of carbon stars. More sensitive observations may, of course, detect SiC_2 emissions at low levels in the inner CSE. Our findings provide new insights into the chemical processes occurring in the CSEs of evolved stars and contribute to our understanding of the chemical evolution of ISM. A further detailed understanding of SiC_2 formation requires studying and comparing more C-rich AGB stars by combining the results of single-dish and high-resolution interferometric observations.

Data availability statement

Publicly available datasets were analyzed in this study. These data can be found in the following: the datasets analyzed for this study can be found in the ALMA Science Archive: https://almascience.nrao.edu. This paper makes use of the following ALMA data: ADS/JAO.ALMA 2013.1.00070.S.

Author contributions

YF prepared the project, processed the ALMA Archive data, and wrote the draft. XL initiated the project, guided the work, and revised the manuscript. TM was involved in interpreting the results, and reviewing and revising the manuscripts. RS provided continuous manuscript revisions. KW provided insights and feedback during the analysis process of the results. FX helped with the data analysis. DQ, SQ, XF, BJ, QC, G-LH, FL, and YZ provided comments and suggestions on the manuscript. JT, ZM, RM, JS, and JY were involved in analyzing the results and provided suggestions for the manuscript. All authors contributed to the article and approved the submitted version.

Funding

XL acknowledges the support from the Xinjiang Tianchi project (2019). TM is grateful to the Leverhulme Trust for the award of an Emeritus Fellowship. This work was also funded by the National Science Foundation of China (12173023), the China Manned Space Project (CMS-CSST-2021-A09), the National Science Foundation of China (11973013), the National Key Research and Development Program of China (22022YFA1603102), the National Natural Science Foundation of China (92261101), the Innovation Capability Support Program of Shaanxi Province (2023-CX-TD-49), and the National Natural Science Foundation of China (11973075). XF, SQ, and YZ thank the Xinjiang Uygur Autonomous Region of China for their support through the Tianchi Talent Program.

Acknowledgments

The authors appreciate the invaluable suggestions of the two reviewers on this work, which has significantly improved the quality of this paper. This paper makes use of the following ALMA data: ADS/JAO.ALMA 2013.1.00070.S. ALMA is a partnership of ESO (representing its member states), NSF (the United States), and NINS (Japan), together with NRC (Canada), MOST and ASIAA (Taiwan), and KASI (the Republic of Korea), in cooperation with the Republic of Chile. The Joint ALMA Observatory is operated by ESO, AUI/NRAO, and NAOJ. The authors are very grateful to Professor Lars-Åke Nyman (the PI of the ALMA project that provided the data for this work) for his valuable comments and suggestions. This research has made use of Astropy[7], a community-developed core Python package for astronomy, and Matplotlib.

Conflict of interest

The authors declare that the research was conducted in the absence of any commercial or financial relationships that could be construed as a potential conflict of interest.

Publisher's note

Supplementary material

The Supplementary Material for this article can be found online at: https://www.frontiersin.org/articles/10.3389/fspas.2023.1215642/full#supplementary-material

References

Agúndez, M., Cernicharo, J., Quintana-Lacaci, G., Castro-Carrizo, A., Velilla Prieto, L., Marcelino, N., et al. (2017). Growth of carbon chains in IRC +10216 mapped with ALMA. *Astron. Astrophys.* 601, A4. doi:10.1051/0004-6361/201630274

Agúndez, M., Cernicharo, J., Quintana-Lacaci, G., Velilla Prieto, L., Castro-Carrizo, A., Marcelino, N., et al. (2015). The peculiar distribution of CH_3CN in IRC +10216 seen by ALMA. *Astrophys. J.* 814, 143. doi:10.1088/0004-637X/814/2/143

Agúndez, M., Fonfría, J., Cernicharo, J., Kahane, C., Daniel, F., and Guélin, M. (2012). Molecular abundances in the inner layers of IRC +10216. *Astron. Astrophys.* 543, A48. doi:10.1051/0004-6361/201218963

Cernicharo, J., Marcelino, N., Agúndez, M., and Guélin, M. (2015). Molecular shells in IRC +10216: tracing the mass loss history. *Astron. Astrophys.* 575, A91. doi:10.1051/0004-6361/201424565

Cernicharo, J., Waters, L., Decin, L., Encrenaz, P., Tielens, A., Agúndez, M., et al. (2010). A high-resolution line survey of IRC +10216 with herschel/hifi-first results: detection of warm silicon dicarbide (SiC). *Astron. Astrophys.* 521, L8. doi:10.1051/0004-6361/201015150

Cherchneff, I. (2006). A chemical study of the inner winds of asymptotic giant branch stars. *Astron. Astrophys.* 456, 1001–1012. doi:10.1051/0004-6361:20064827

Danilovich, T., Ramstedt, S., Gobrecht, D., Decin, L., De Beck, E., and Olofsson, H. (2018). Sulphur-bearing molecules in agb stars-ii. abundances and distributions of CS and SiS. *Astron. Astrophys.* 617, A132. doi:10.1051/0004-6361/201833317

De Beck, E., and Olofsson, H. (2020). The surprisingly carbon-rich environment of the S-type star W Aql 642. *Astron. Astrophys.*, A20. doi:10.1051/0004-6361/202038335

Decin, L., Cherchneff, I., Hony, S., Dehaes, S., De Breuck, C., and Menten, K. M. (2008). Detection of "parent" molecules from the inner wind of AGB stars as tracers of non-equilibrium chemistry. *Astron. Astrophys.* 480, 431–438. doi:10.1051/0004-6361:20078892

Decin, L. (2021). Evolution and mass loss of cool aging stars: a daedalean story. *Annu. Rev. Astron. Astrophys.* 59, 337–389. doi:10.1146/annurev-astro-090120-033712

Decin, L., Richards, A. M. S., Neufeld, D., Steffen, W., Melnick, G., and Lombaert, R. (2015). ALMA data suggest the presence of spiral structure in the inner wind of CW Leonis. *Astron. Astrophys.* 574, A5. doi:10.1051/0004-6361/201424593

Fonfría, J. P., Fernández-López, M., Agúndez, M., Sánchez-Contreras, C., Curiel, S., and Cernicharo, J. (2014). The complex dust formation zone of the AGB star IRC +10216 probed with CARMA 0.25 arcsec angular resolution molecular observations. *Mon. Notices Royal Astron. Soc.* 445, 3289–3308. doi:10.1093/mnras/stu1968

Gensheimer, P. D., Likkel, L., and Snyder, L. E. (1995). Full synthesis maps of circumstellar SiC_2 in IRC +10216. *Astrophys. J.* 439, 445. doi:10.1086/175186

Glassgold, A. E., Lucas, R., and Omont, A. (1986). Molecular ions in the circumstellar envelope of IRC +10216. *Astron. Astrophys.* 157, 35–48.

---

[7] www.astropy.org

Glassgold, A. E., Mamon, G. A., and Huggins, P. J. (1991). The formation of molecules in protostellar winds. *Astrophys. J.* 373, 254–265. doi:10.1086/170045

Gong, Y., Henkel, C., Spezzano, S., Thorwirth, S., Menten, K., Wyrowski, F., et al. (2015). A 1.3 cm line survey toward IRC +10216. *Astron. Astrophys.* 574, A56. doi:10.1051/0004-6361/201424819

Groenewegen, M., Sevenster, M., Spoon, H., and Pérez, I. (2002). Millimetre observations of infrared carbon stars. mass loss rates and expansion velocities. *Astron. Astrophys.* 390, 511–522. doi:10.1051/0004-6361:20020728

Guelin, M., Lucas, R., and Cernicharo, J. (1993). MgNC and the carbon-chain radicals in IRC +10216. *Astron. Astrophys.* 280, L19–L22.

Höfner, S., and Olofsson, H. (2018). Mass loss of stars on the asymptotic giant branch. *Astron. Astrophys. Rev.* 26, 1–92. doi:10.1007/s00159-017-0106-5

Li, X., Millar, T. J., Heays, A. N., Walsh, C., van Dishoeck, E. F., and Cherchneff, I. (2016). Chemistry and distribution of daughter species in the circumstellar envelopes of O-rich AGB stars. *Astron. Astrophys.* 588, A4. doi:10.1051/0004-6361/201525739

Li, X., Millar, T. J., Walsh, C., Heays, A. N., and Van Dishoeck, E. F. (2014). Photodissociation and chemistry of N_2 in the circumstellar envelope of carbon-rich agb stars. *Astron. Astrophys.* 568, A111. doi:10.1051/0004-6361/201424076

Lucas, R., Guélin, M., Kahane, C., Audinos, P., and Cernicharo, J. (1995). Plateau de bure observations of IRC +10216: high sensitivity maps of SiC_2, SiS, CS. *Astrophys. Space Sci.* 224, 293–296. doi:10.1007/BF00667860

Lykou, F., Zijlstra, A. A., Kluska, J., Lagadec, E., Tuthill, P. G., Avison, A., et al. (2018). The curious case of II Lup: a complex morphology revealed with SAM/NACO and ALMA. *Mon. Not. R. Astron. Soc.* 480, 1006–1021. doi:10.1093/mnras/sty1903

MacKay, D. D. S., and Charnley, S. B. (1999). The silicon chemistry of IRC+10°216. *Mon. Notices Royal Astron. Soc.* 302, 793–800. doi:10.1046/j.1365-8711.1999.02175.x

Massalkhi, S., Agúndez, M., Cernicharo, J., Velilla Prieto, L., Goicoechea, J. R., Quintana-Lacaci, G., et al. (2018). Abundance of SiC_2 in carbon star envelopes. *Astron. Astrophys.* 611, A29. doi:10.1051/0004-6361/201732038

Müller, H. S. P., Schlöder, F., Stutzki, J., and Winnewisser, G. (2005). The cologne database for molecular spectroscopy, CDMS: a useful tool for astronomers and spectroscopists. *J. Mol. Struct.* 742, 215–227. doi:10.1016/j.molstruc.2005.01.027

Nyman, L.-Å., and Olofsson, H. (1995). Molecular abundances in carbon-rich circumstellar envelopes. *Astrophys. Space Sci.* 224, 527–528. doi:10.1007/bf00667938

Prieto, L. V., Cernicharo, J., Quintana-Lacaci, G., Agúndez, M., Castro-Carrizo, A., Fonfría, J. P., et al. (2015). Si-bearing molecules toward IRC +10216: ALMA nuveils the molecular envelope of cwleo. *Astrophys. J. Lett.* 805, L13. doi:10.1088/2041-8205/805/2/l13

Ramstedt, S., Schöier, F. L., and Olofsson, H. (2009). Circumstellar molecular line emission from S-type AGB stars: mass-loss rates and SiO abundances. *Astron. Astrophys.* 499, 515–527. doi:10.1051/0004-6361/200911730

Smith, C. L., Zijlstra, A. A., and Fuller, G. A. (2015). A molecular line survey of a sample of AGB stars and planetary nebulae. *Mon. Notices Royal Astron. Soc.* 454, 177–200. doi:10.1093/mnras/stv1934

Takano, S., Saito, S., and Tsuji, T. (1992). Silicon chemistry in the outer envelope of IRC +10216: the detailed distribution of SiC_2. *Publ. Astron. Soc. Japan* 44, 469–480.

Thaddeus, P., Cummins, S. E., and Linke, R. A. (1984). Identification of the SiCC radical toward IRC +10216: the first molecular ring in an astronomical source. *Astrophys. J.* 283, L45–L48. doi:10.1086/184330

Van de Sande, M., and Millar, T. J. (2022). The impact of stellar companion UV photons on the chemistry of the circumstellar environments of AGB stars. *Mon. Notices Royal Astron. Soc.* 510, 1204–1222. doi:10.1093/mnras/stab3282

Velilla-Prieto, L., Cernicharo, J., Agúndez, M., Fonfría, J. P., Castro-Carrizo, A., Quintana-Lacaci, G., et al. (2018). Circumstellar chemistry of Si-C bearing molecules in the C-rich AGB star IRC +10216. *Proceedings of the International Astronomical Union* 14, 535–537. doi:10.1017/s1743921318005410

Wang, K., Zhang, Q., Testi, L., van der Tak, F., Wu, Y., Zhang, H., et al. (2014). Hierarchical fragmentation and differential star formation in the galactic 'snake': infrared dark cloud g11.11-0.12. *Mon. Notices Royal Astron. Soc.* 439, 3275–3293. doi:10.1093/mnras/stu127

Willacy, K., and Cherchneff, I. (1998). Silicon and sulphur chemistry in the inner wind of IRC +10216. *Astron. Astrophys.* 330, 676–684.

Woods, P., Schöier, F. a., Nyman, L.-Å., and Olofsson, H. (2003). Molecular abundances in carbon-rich circumstellar envelopes. *Astron. Astrophys.* 402, 617–634. doi:10.1051/0004-6361:20030190

Yang, T., Bertels, L., Dangi, B. B., Li, X., Head-Gordon, M., and Kaiser, R. I. (2019). Gas phase formation of c-SiC_3 molecules in the circumstellar envelope of carbon stars. *Proceedings of the National Academy of Science* 116, 14471–14478. doi:10.1073/pnas.1810370116

Zhang, Y., Kwok, S., Dinh-V-Trung, (2009). A molecular line survey of the highly evolved carbon star CIT 6. *Astrophys. J.* 691, 1660–1677. doi:10.1088/0004-637x/691/2/1660